

ED PROCEEDINGS OF THE 7TH INT'L CRYOGENIC ENGINEERING CONFERENCE
SAFETY ASPECTS FOR LHe CRYOSTATS AND LHe TRANSPORT CONTAINERS - LONDON 4-7 JULY
1978

W. Lehmann, G. Zahn

Kernforschungszentrum Karlsruhe, Institut für Technische Physik, 7500 Karlsruhe, FRG

Venting of the vacuum jacket surrounding a LHe vessel with atmospheric air is a serious interference. Depending on construction and insulation design of the apparatus a heat flow into the LHe up to some W/cm^2 may occur. Condensation and freezing of the air initiates a quick evaporation of the LHe bulk.

The LHe vessels of cryostats and containers are pressure tanks and must therefore be provided with sufficiently dimensioned safety devices.

We present the results of air exposure experiments which have been performed with standard laboratory cryostats and a 100 l standard LHe container. Results of several blow down experiments will be discussed and compared. They give realistic data for the layout of safety devices of such He-containers. The scalability to He tanks in general will be discussed.

1. INTRODUCTION

Liquid helium cryostats and liquid helium storage containers are high vacuum insulated and, in most cases, superinsulated. Evacuation to a pressure $<10^{-5}$ mbar reduces the heat input to the liquid helium by approximately a factor of 100, the use of a superinsulation reduces it by another factor of 10. The installation of shields cooled by helium return gas or liquid nitrogen in the insulating vacuum reduces further the heat input to the liquid helium bath. If these techniques are applied, liquid helium equipments with very low loss rates can be built.

A breakdown of the insulating vacuum results in a corresponding increase in losses and also entails hazards which should not be underestimated. Specially because of the low heat of vaporization, the large temperature difference relative to the atmosphere and the enormous density changes which may occur, a liquid helium vessel must be protected in general against the "destruction of the insulating vacuum" incident by proper design and by the installation of blowdown systems.

2. POTENTIAL DEFECTS ARISING IN THE OPERATION OF LIQUID HELIUM DEWARS

The following outline relates to defects that should generally be considered in designing safety systems (blowdown systems) of liquid helium containers and helium bath cryostats. Incidents which may be caused by cryostat installation (such as quenching of a magnet, defocusing of an energy beam, high voltage flash-over etc.) will not be covered. They may, under certain conditions, give rise to even higher thermal load of the liquid helium bath and must therefore be taken into account specifically in the light of each case.

An increased heat input into the liquid helium bath, compared with normal operation, may be due to the following conditions:

- leaking helium tank (minor leakage)
- damage to helium tank
- leaking liquid nitrogen cold shield (minor leakage)
- damage to liquid nitrogen cold shield
- leaking outer tank (minor leakage)
- damaged outer tank

- upset thermodynamical equilibrium conditions in the helium tank
- Thermal oscillations in the helium tank.

The theoretically possible effects of such failures in LHe-vessels and -cryostats of the usual sizes and designs have been analyzed. Assumptions and results are collected in Table 1. Calculations have been done under the condition that the helium tank is located in an environment of approximately 80 K which, in practice, is brought about by cold shields.

Table 1. Comparison of incidents within a LHe dewar. Estimation of heat load which may occur.

| Reasons for an increased heat load | Assumptions | computed maximum heat flux q [W/cm ²] | comments |
|--|--|---|---|
| <u>Leaking He-tank</u> | a) stagnant He-Gas | 0.02 (p=1bar) | $\lambda_{He} = f(p,s)$ acc. to Fig. 1 and to inform. in [1] |
| | b) free convection of He-Gas at the vertical walls of the vessel $Nu=0.10(Gr \cdot Pr)^{1/3}$ | 0.25 (p=1bar) | H = 0.8 m, $\Delta T = 75$ K acc. to [2] |
| | c) actual conditions in LHe-dewars | 0.02-0.25 (p=1bar) | Reality between a) and b) Influence of different conditions for convection of gas acc. to Fig. 1 |
| <u>Damage to He-tank</u> | LHe leaking out into insulation space. p=1bar in both rooms. Film boiling | (5-25) (p=1bar) | theoretical peak values, locally and temporary, $\Delta T_{wall-LHe} = 80-300$ K |
| <u>Leaking LN₂-shield or outer tank</u> | heat input due to radiation, heat conduction and condensation of air at p=10 ⁻⁶ mbar: 10 ⁻⁴ W/cm ² | 0.01 (p=10 ⁻⁴ mbar) | Cryopumping effect retains vacuum. Increase of heat flux due to condensation. acc. to [6] |
| <u>Damage to LN₂-shield or outer tank</u> | Film condensation at vertical walls $\alpha_{lam} = 0.943 \left(\frac{g \cdot \lambda \cdot \rho \cdot r}{H \cdot \Delta T \cdot \eta} \right)^{1/4}$ $\alpha_{turb} = 0.003 \left(\frac{H \cdot \Delta T \cdot g \cdot \lambda \cdot \rho \cdot r}{r \cdot \eta^3} \right)^{1/2}$ | 2-3 (p=1bar) uninsulated tank 0.5 (p=1bar) superinsulated tank | acc. to [2] Steady state saturated N ₂ -vapor. Linear temp.-gradient within the film function of ice layer acc. to [7] |
| <u>Thermal Stratification</u> | usual handling of LHe-cryostats and LHe-laboratory containers | comparatively minor heat input | severe incidents unlikely. Motion of the liquid prevents building up of stratification |
| <u>Thermal oscillation</u> | quarter-wave-length standing wave | comparatively minor heat input (some W up to some 100 W max.) | incident can be avoided by proper design of the LHe dewar and the installations. |

3. EXPERIMENTAL

Calculated estimates of incidents (table) and results are collected in the most serious. For the following:

- In reality it is a condensate involved.
- There is no balancing process.
- The assumed conditions for the liquid level are limited.
- So far only tested. At the time of the experiment, it gave rise to

The effect of other conditions and equipment

Without simplification within a mean value. At the other hand, it is the most dangerous. This may happen in helium dewars.

In order to check the safety system during experiments of the safety particle separator, quantitative measurements and experiments

Test program:

1. Venting of a cooled helium dewar
2. Venting of a cooled helium dewar
3. Venting of a cooled helium dewar

In addition to the helium dewar, radio frequency superconducting

4. Venting of a cooled helium dewar

The experiments were the first, but no flow, but no ping from the measuring system. The mass flow through the tank). During changes quick

3. EXPERIMENTAL PROGRAM

Calculated estimates of the heat input into the liquid helium bath as a result of incidents (table 1) are based on a number of simplifying assumptions, especially in the most serious case of "venting the insulation vacuum with atmospheric air". For the following reasons, these estimates can only be crude approximations:

- In reality it is not condensation of a stagnant pure type of saturated vapor, but a condensation and melting event of several components of atmospheric air that is involved.
- There is no steady-state but an initially non-steady-state influx and temperature balancing process.
- The assumed data for the condensate and the ice, the heat transfer coefficients to the liquid helium and the temperature gradients in the "insulating layers" are of limited accuracy only.
- So far only the heat transfer on the vertical walls of the tanks has been calculated. At the horizontal bottom it is possible for condensate to drip, which may give rise to higher heat flux densities in that area.

The effect of such an incident depends on boundary conditions mentioned above and on other conditions whose effect is difficult to estimate, such as the physical design and equipment of the liquid helium tank and the vacuum space.

Without simplifications it is hardly possible to estimate the complex events involved within a meaningful expenditure of computation effort.

At the other hand the sudden venting of the insulating vacuum with atmospheric air is the most dangerous accident which can occur in normal (laboratory) operation. This may happen as a result of mal operation or damage to the outer tank of liquid helium dewars.

In order to clarify the true situation, and as a necessary basis for the design of safety systems for liquid helium tanks and cryostats, we therefore carried out "venting experiments". Actual a reason for this work was the need for a failsafe design of the safety systems for the two large helium II cryostats of the superconducting particle separator for SPS/CERN [8]. The test program was designed in such a way that quantitative heat flux densities were obtained for different insulation conditions and existing standard tanks could be used.

Test program:

1. Venting of a liquid helium cryostat with liquid nitrogen cold shield and uninsulated helium tank.
2. Venting of a liquid helium cryostat with liquid nitrogen cold shield and superinsulated helium tank.
3. Venting of a liquid helium transport container with superinsulated and returning cooled cold shields.

In addition to these tests, which served to clarify primary defects on the liquid helium dewar, one experiment was carried out to analyze an incident occurring in the radio frequency superconductivity technology (breakdown of the beam vacuum within a superconducting cavity):

4. Venting of a liquid helium bath cooled niobium deflector (normally UHV pumped).

The experiments were carried out on "open" tanks because the primary points of interest were the thermal load of the helium tanks and the resultant maximum helium mass flow, but not the increase in pressure. Thus, the whole mass of helium offgas escaping from the tank could be measured continuously and moved through the mass flow measuring section open towards the atmosphere. In addition, it was possible to verify the mass flow measurement in an integral way by means of superconducting static probes through the level measurement at the beginning and in the end of venting (emptying tank). During the main phase of venting this level indication did not respond to changes quickly enough.

4. TEST SETUP AND EVALUATION OF MEASUREMENTS

The basic setup of the experiment and the test objects with their main data can be seen from Fig. 3.1 to 3.5. Before the insulation vacuum was vented, the tanks were in a thermal equilibrium at an insulation vacuum $<10^{-5}$ mbar. Venting with atmospheric air was done by means of a remotely operated solenoid valve V (ND = 50 mm) and a short connecting line (ND = 32 mm). The helium vaporizing as a result of the heat input was led into the open air through the measuring section with an orifice sketched in Fig. 3.5 in more detail and designed according to DIN 1952 [9], and the escaping helium mass flow was determined. During the venting process the liquid helium level, the temperatures and the pressures listed in Fig. 3.5 were recorded by means of compensographs.

The temperature sensors attached to the standard orifice did not respond to changes quickly enough; for this reason, the temperature of the helium gas at this point was calculated in a computation procedure by using the sensors at the inlet and outlet and assuming a logarithmic temperature development.

Calculation of the helium mass flow through the VDI-Norm-orifice was done by the relation indicated in [9,10] and derived from the energy and continuity equation.

The density and the dynamic viscosity of the helium upstream of the orifice were determined by means of the Heltherm Program of the National Bureau of Standards. The computer program used to evaluate the measured data determines the mass flow \dot{m} in several iteration steps. For the first run a Reynolds number of 10^5 was assumed. If the difference between the assumed Reynolds number and the Reynolds number as determined from the mass flow measurement was $<10\%$, the iteration process was terminated.

The reference for the heat input into the liquid helium bath is the vaporization rate. This is not identical with the helium mass flow leaving the cryostat, because pressure, temperature, liquid and gas volumes and, hence, the mass of helium stored in the gas space, changed during the experiment. The mass flow actually vaporized is:

$$\dot{m}_v = \frac{\rho_{LHe}}{\rho_{LHe} - \rho_{gHe}} \cdot (\dot{m} + v_{gHe} \cdot \frac{\Delta p_{gHe}}{\Delta t})$$

↑ THRU ORIFICE

The heat input (\dot{Q}) and the heat flux density (q) to the liquid helium bath can then be determined as follows:

$$\dot{Q}_{LHe} = \dot{m}_v \cdot r; \quad q = \dot{Q}_{LHe} / A_{LHe}$$

To determine the heat exchange area A_{LHe} in the measurements the computer program calculated the mass of helium vaporized in the cryostat between two points in time and, hence, the decrease in the level. This value was always subtracted from the previous liquid helium level and thus indicated the instantaneous liquid helium level. To calculate the heat exchange area wetted by liquid helium the mean value of the liquid helium levels between two points in time were used by the computer program.

5. MEASURED RESULTS AND DISCUSSION

Fig. 4 shows the development as a function of time of the interesting quantities \dot{m}_v , q and Δp during venting of the insulating vacuum of the bath cryostat with an uninsulated helium tank as shown in Fig. 3.1. The specific heat input per unit area q_v rose to the remarkable peak of approx. 3.8 W/cm^2 within some 6 s and then dropped again as a result of the increasing insulation effect of the air-ice layer forming. After some 20 s the liquid helium tank was empty. The earlier and more marked decrease of vaporized helium \dot{m}_v is explained by the increasing insulating action accompanied by a decreasing heat exchange area brought about by the reduction in the liquid helium level.

Fig. 5 shows the comparison of the results when venting an uninsulated bath cryostat and one superinsulated according to Fig. 3.2. The enormous protective action of the superinsulation in these incidents is evident. It not only represents a static insu-

lation layer, but by convection.

Fig. 5 also show helium transport of all experimen

The protective a case of the liqu in a comparison tanks. After son 70 l of liquid h

Fig. 6 shows a c uninsulated heli ting in liquid l

Fig. 7 shows the parison with est tion between the change areas of

The fact that tl primarily explai of the air mixt tionary ("stagn Moreover it mus can be even muc in an ice layer

The tank pressu heat input (Fig always open to and the install

However it shou tainers are clo occur under inc system properly

Atmospheric moi lead to a close nitrogen tanks

The pressure bu filling level c and the initial

Table 2. Isochr

| Part of liquid [Vol. %] | |
|-------------------------|-------|
| 100 | (100) |
| 60 | (5) |
| 0 | (0) |

lation layer, but also prevents the direct access of incoming air and a heat transfer by convection.

Fig. 5 also shows the results of the venting tests carried out on the 100 l liquid helium transport container, thus constituting an overall description and comparison of all experiments in which the insulating vacuum had been vented.

The protective action of the cold shields surrounding the liquid helium tank in the case of the liquid helium transport container (according to Fig. 3.3) becomes visible in a comparison with the results of the uninsulated and the superinsulated helium tanks. After some 60 s the transport vessel, which had initially been filled with 70 l of liquid helium, was empty.

Fig. 6 shows a comparison of the results obtained in venting the cryostat with an uninsulated helium tank and those obtained when venting the niobium deflector floating in liquid helium.

Fig. 7 shows the summary of the measured and calculated maximum heat input and a comparison with estimates known from the literature [11]. Moreover it gives a correlation between the maximum heat input which must be expected for different heat exchange areas of similar LHe dewars.

The fact that the measured values are partly much higher than the computed ones is primarily explained by the fact that the heat transfer by condensation and freeze-out of the air mixture in a non-steady-state venting process was assumed to be too stationary ("stagnant saturated nitrogen vapor").

Moreover it must be mentioned that the discrepancies between computation and reality can be even much higher depending on the assumptions for heat transmission especially in an ice layer and to the LHe bath.

The tank pressure, which occurred in all experiments and increased with the specific heat input (Fig. 5,6), was low as a result of the fact that the measuring line was always open to the atmosphere. This was a quasi-isobar change of state (vaporization) and the installed safety valves were never actuated.

However it should be mentioned that normally cryostats and liquid helium storage containers are closed pressure vessels in which considerable pressure increases can occur under incident conditions, which may cause the vessel to burst unless a safety system properly dimensioned can be actuated.

Atmospheric moisture freezing out in a venting line open to the atmosphere, may also lead to a closed pressurized tank and to a potential hazard, especially in liquid nitrogen tanks or shields.

The pressure buildup theoretically possible is very much dependent on the initial filling level of the vessel or, to put it differently, on the initial vapor content and the initial density of the mixture, respectively (Table 2).

Table 2. Isochoric change of state for Helium (for Nitrogen resp.)

| Part of liquid [Vol. %] | X_1 | $P_{(T=10\text{ K})}$ [bar] | $P_{(T=300\text{ K})}$ [bar] |
|----------------------------|-----------|-----------------------------|------------------------------|
| 100 (100) | 0 (0) | 28 | 1300 (3000) |
| 60 (5) | 0,1 (0,1) | 13 | 400 (42) |
| 0 (0) | 1 (1) | 3,3 | 100 (4,5) |

6. SCALABILITY OF RESULTS

In liquid helium dewars of the type studied here turbulent film condensation must be assumed on the side walls with heights >0.7 m under the simplified and mentioned assumption of an exclusive nitrogen condensation. If the height is doubled, a 40 % increase in the coefficient of heat transfer can be expected in this range of state ($\alpha_{\text{turb}} \sim \sqrt{H}$).

At border conditions (height $H = 0.7$ m) computations according to the equations of section 2 lead to approximately 20 % higher values for turbulent conditions compared with laminar ones.

At vessel heights <0.7 m laminar film condensation will result in an increase of the heat transfer coefficients with decreasing heights. This results for instance in an increase of appr. 10 % at a height of 0.5 m and in a further increase of appr. 20 % with a further bisection of the height of the tank ($\alpha_{\text{lamin}} \sim H^{-1/4}$).

The physical location of the liquid helium tank also influences the heat transfer conditions by condensation. Because of the short runs, laminar film condensation must be expected to occur on horizontal tanks. In the dimensions of Length/Diameter $\approx 1:5$ customary in LHe-tank designs the heat transfer coefficients α_{lam} to be expected are assumed to be approx. 20 % lower up to 20 % higher than in vertical tank arrangements (according to information in [2]).

These considerations result in the conclusion that the heat transfer conditions within the film of condensation do not deviate more than approximately 40 % for usual LHe dewar design neither for vertical nor for horizontal type. Even in case of uninsulated thin cryovessels the heat transfer and the possible heat flux to the LHe bath is influenced strongly by the heat barriers inside an air ice layer, inside the SS-tank and at the border to the LHe. Therefore the influence of size and position of the LHe tank on the interesting heat flux to the bath (\dot{q}) will be relatively unimportant ($<4+20$ % for the discussed field).

So, the experimental results, summarized in Fig. 7, can be a base for scaling the maximum heat input to similar dewars with modified sizes.

If the liquid helium tanks are thick walled and/or thermally insulated, the heat loads generated by a penetration of atmospheric air will be greatly reduced relative to the extreme case of the uninsulated thin vessel, because in that case the insulating layer greatly influence the heat transmission to the liquid helium. A good basis of assessment could be represented by the measurements mentioned above with and without superinsulation. Ten layers of superinsulation in that case already resulted in a reduction of the incident heat to 16 % (Fig. 7). A rough calculation in determining the heat transfer coefficient is possible under the assumption of an insulation value in the vented superinsulation which is equal to that of stagnant nitrogen gas at atmospheric pressure. However, this can apply only if the superinsulation is directly attached to the liquid helium tank and direct contacts of the tank with air are prevented.

7. CONCLUSION

For liquid helium transport containers and liquid helium cryostats venting of the insulating vacuum by atmospheric air or nitrogen from a liquid nitrogen cold shield represents the gravest "natural incident" under normal conditions. (Fire in the immediate vicinity of the cryovessels and extreme energy released by internals in cryostats were excluded). Depending on the insulation and the accessibility of the liquid helium tanks to air there may be short term peak heat loads of up to several W/cm^2 of liquid helium exchange area.

Because of the complex non-steady-state behaviour and, hence, the difficulty to calculate events accompanying condensation and freeze-out of the air and the heat transfer to liquid helium, model experiments were carried out on liquid helium standard dewars to verify computed estimates. The experiments performed in the following maximum specific heat loads (and blowdown rates, respectively):

Table 3. Max

| | |
|-----|------|
| 0.6 | W/cm |
| 2 | W/cm |
| 3.8 | W/cm |
| 1.8 | W/cm |

The discrepancy in computation is higher. All range of estimates as possible as The results other measurements reduce the statistics and list of reasonable submitted is

LIST OF SYMBOLS

| | |
|---|--|
| Nu | = $\alpha \cdot H / \dots$ |
| Gr | = $g \cdot H^3$ |
| Pr | = $\eta \cdot c_p$ |
| H | = height |
| g | = acceleration |
| $\alpha_{\text{lamin}}, \alpha_{\text{turb}}$ | = heat transfer coefficients |
| c_p | = specific heat |
| r | = late |
| \dot{m}_v | = helium vaporization rate |
| \dot{m} | = helium mass flow |
| v | = mean velocity |
| ρ_{LHe} | = density of liquid helium |
| ρ_{gHe} | = density of gaseous helium |
| Δt | = temperature difference |
| $\Delta \rho_{\text{gHe}}$ | = density difference of gaseous helium |

Table 3. Maximum heat flux and blowdown rates for the tested objects

| | | |
|-----|--|---|
| 0.6 | W/cm^2 (≈ 0.03 g/s cm^2) | for the superinsulated tank of a bath cryostat |
| 2 | W/cm^2 (≈ 0.1 g/s cm^2) | for a liquid helium transport container equipped with offgas cooled shields |
| 3.8 | W/cm^2 (≈ 0.2 g/s cm^2) | for an uninsulated tank of a bath cryostat |
| 1.8 | W/cm^2 (≈ 0.1 g/s cm^2) | for the liquid helium flooded deflector model |

The discrepancy between the computed estimate and the measured values is most pronounced in the uninsulated tank of the cryostat. Compared with the greatly simplified computation setups, the measured results led to values approximately 20 up to 80 % higher. All computed and experimental results can easily be fit into the general range of estimated values quoted in [11] (Fig. 7). Scaling of our experimental results to other sizes of similar LHe dewars seems to be possible as far as the remarks of section 6. are considered. The results clearly show that careful insulation of the liquid helium tank or some other measure taken to prevent the admission of air to the liquid helium can greatly reduce the penetration of heat in venting the insulating vacuum. Liquid helium cryostats and liquid helium transport containers can then be equipped with safety systems of reasonable dimensions. The design of such systems on the basis of the guidelines submitted is possible, e.g., according to [11, 12].

LIST OF SYMBOLS

| | | | | |
|-------------------------------|---|-----------------|--|--|
| Nu | $= \alpha \cdot H / \lambda$ | Nusselt number | λ | = thermal conductivity [W/m K] |
| Gr | $= g \cdot H^3 \cdot \rho^2 \cdot \Delta T \cdot \frac{\beta}{\eta^2}$ | Grashof number | η | = dynamic viscosity [Pa s] |
| Pr | $= \eta \cdot c_p / \lambda$ | Prandtl number | ρ | = density [kg/m^3] |
| H | = height of LHe-tank [m] | | β | = coefficient of thermal expansion [1/K] |
| g | = acceleration constant [m/s^2] | | ΔT | = temperature difference [K] |
| $\alpha_{lam}, \alpha_{turb}$ | = heat transfer coefficient at laminar, turbulent film conditions [$W/m^2 K$] | | | |
| c_p | = heat capacity at p=const. [J/kg K] | \dot{Q}_{LHe} | = heat load to LHe [W] | |
| r | = latent heat of vaporization [J/kg] | \dot{q} | = \dot{Q}_{LHe} / A_{LHe} heat flux density [W/cm^2] | |
| \dot{m}_v | = helium mass flow actually vaporized | A_{LHe} | = area of heat exchange with the LHe | |
| \dot{m} | = He mass flow through orifice | X_1 | = (mass vapour)/(mass mixture) in the LHe-tank at the beginning of isochoric change of state | |
| v_{gHe} | = mean gas volume in He-tank between two points of time | | | |
| ρ_{LHe} | = density of LHe | | | |
| ρ_{gHe} | = density of gaseous He with PR1 and the assumption of an arithmetic temperature mean between TR1 and the vaporization temperature (Fig. 3) | | | |
| $\Delta \tau$ | = difference in time between two measurements | | | |
| $\Delta \rho_{gHe}$ | = density difference between two successive points in time | | | |

REFERENCES

- [1] Hofmann, A. 'Messungen der Wärmeleitfähigkeit von Pulvervakuumisolierungen'. Linde-Berichte aus Technik und Wissenschaft, 19/1965.
- [2] VDI-Wärmeatlas, Berechnungsblätter für den Wärmeübergang, VDI-Verlag, 1974.
- [3] Probert, S.D. 'Thermal Insulation', Elsevier publishing Co. Ltd., 1968.
- [4] Smoluchowski, M., Ber. II, Internationaler Kältekongreß, Wien, 1910.
- [5] Smith, R.V. 'Review of heat transfer to helium I'. Cryogenics, Februar 1969.
- [6] Wutz, M. 'Theorie und Praxis der Vakuumtechnik', Verlag Friedrich Vieweg u. Sohn, Braunschweig, 1965.
- [7] Cock, T. and Davey, G. 'The density and thermal conductivity of solid nitrogen and carbon dioxide, Cryogenics, June 1976.
- [8] Barth, W. and Lehmann, W. 'Experience with two large-scale HeII-cryostats for a superconducting r.f. particle separator working in closed cycle with a 300 W refrigerator', Proceedings of ICEC 6, Grenoble, 1976.
- [9] Deutsche Normen DIN 1952, Durchflußmessung mit genormten Düsen, Blenden und Venturidüsen, August 1971.
- [10] VDI-Richtlinien, VDI 2040, Durchflußzahlen und Expansionszahlen genormter Drosselgeräte und Abweichungen von den Normvorschriften, Oktober 1971.
- [11] Kropschot, R.H., Birmingham, B.W., Mann, D.B., Editors, 'Technology of Liquid Helium', NBS Monograph 111, October 1968.
- [12] AD-Merkblätter A1 und A2 der Arbeitsgemeinschaft Druckbehälter, 1975 u. 1977.

10'
10'
10'
10'
10'
10'

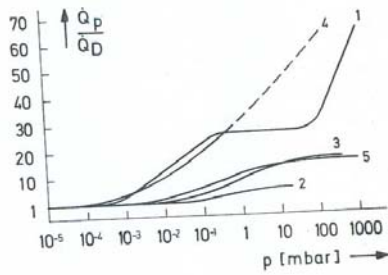
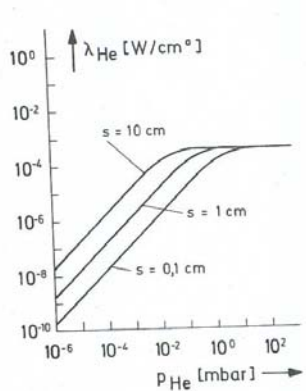
$T_w = 80 K$

Accommo

Fig. 1:

↑
m³ [g/s]

Fig. 4:



$T_W = 80$ K $T_C = 4,2$ K $T_m = 42,1$ K
 Accommodation coefficient of the system = 0,5

- \dot{Q}_D = heat input at design pressure
- 1 5l LO₂ Dewar, void [3]
 - 2 5l LO₂ Dewar, slag wool [3]
 - 3 LN₂ Dewar, Perlit powder
 - 4 large-scale He II cryostat with superinsulation and LN₂ shield [4]
 - 5 Glass wool insulation [4]

Fig. 1: Therm. conductivity of He as function of pressure and wall distance

Fig. 2: Quality of insulation as a function of pressure p

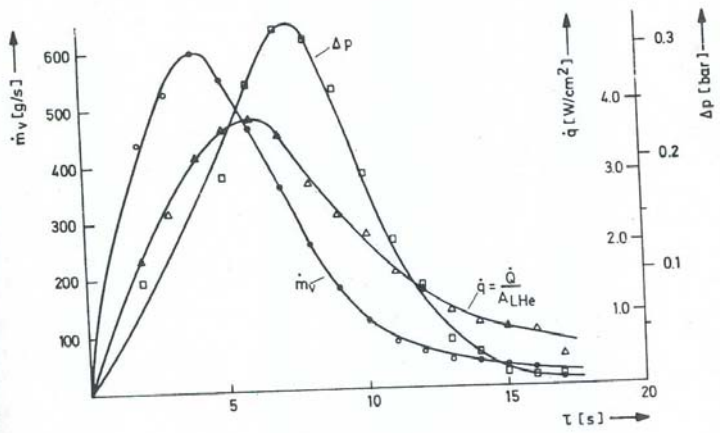


Fig. 4: Air exposure experiment. Cryostat without superinsulation according to Fig. 3.1

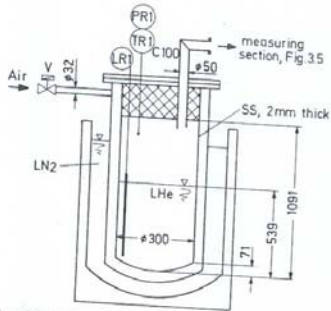


Fig. 3.1 LHe bath cryostat without superinsulation

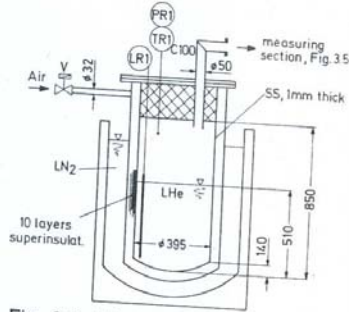


Fig. 3.2 LHe bath cryostat with superinsulation

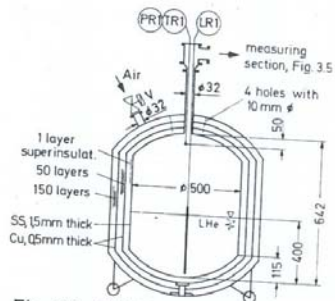


Fig. 3.3 100l LHe container with 2 radiation shields

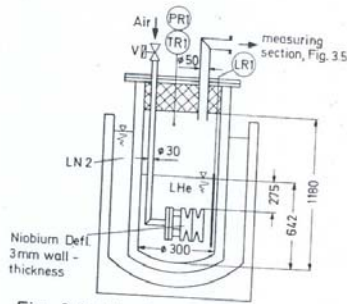


Fig. 3.4 LHe bath cryostat with immersed Niobium Deflector

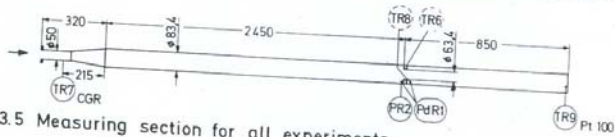
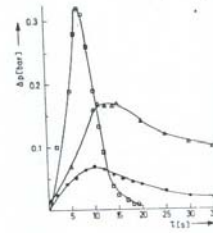
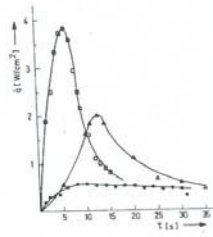


Fig. 3.5 Measuring section for all experiments

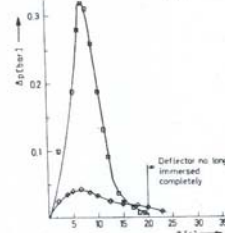
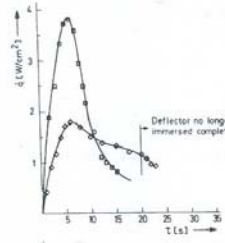
Fig. 3: Experimental objects and testing installations

Fig. 7: S
w



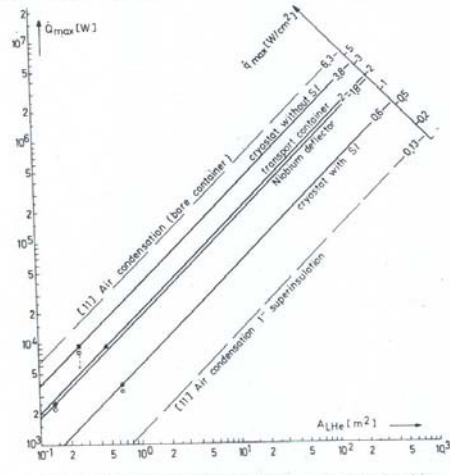
○ Cryostat without superins. according to Fig. 3.1
 ● Cryostat with superinsul. according to Fig. 3.2
 ▲ LHe transport container according to Fig. 3.3

Fig. 5: Air exposure experiments. Comparison of the results



○ Cryostat without superinsulation according to Fig. 3.1
 ● Deflector according to Fig. 3.4

Fig. 6: Air exposure experiments. Comparison of the results



■ Cryostat without superinsulation (○ calculated), ▲ LHe transport container,
 ● Cryostat with superinsulation (○ calculated), ◆ Niob. deflector (○ calculated)

Fig. 7: Scaled heat load based on measurements with the test objects. Comparison with our calculations and estimations of [11].